



# Criegee + HONO reaction: the dominant sink of Criegee, and the missing non-photolytic source of OH<sup>•</sup>

Pradeep Kumar<sup>1</sup>, Vishva Jeet Anand<sup>1</sup>, and Philips Kumar Rai<sup>1</sup>

<sup>1</sup>Department of Chemistry, Malaviya National Institute of Technology Jaipur, Jaipur, 302017, India

**Correspondence:** Pradeep Kumar (pradeep.chy@mnit.ac.in)

- 1 Abstract. One of the most important puzzles in atmospheric chemistry is a mismatch between observed and modelled con-
- 2 centrations of OH<sup>•</sup>/HO<sup>•</sup> in the presence of high concentration of volatile organic compounds. It is now well established that
- 3 to fulfill this gap, one needs a reaction that is not only capable of producing OH• but also able to act as a sink of HO<sub>2</sub>. In
- 4 the present work, we are proposing the Criegee + HONO reaction as a possible solution of this puzzle. Our quantum chemical
- 5 and kinetic calculations clearly suggest that this reaction can not only be an important source of OH radical but can also act
- 6 as a sink of HO<sub>2</sub> radical. Our study also suggests that HONO has the potential to become the most dominant sink of Criegee
- 7 intermediate, surpassing SO<sub>2</sub> and water dimer, even in high humid conditions.

## 8 1 Introduction

It is well-known that the atmospheric chemistry is mainly dominated by the radicals (Anderson, 1987; Monks, 2005). Particularly in the troposphere, these radicals are key in degrading various pollutants, a phenomenon as important as the ozone layer 10 for the existence of life (Weinstock, 1969; Lelieveld et al., 2004). The primary radicals responsible for the oxidative power of 11 troposphere come from the  $HO_X$  (OH $^{\bullet}$ , HO $^{\bullet}$ , RO $^{\bullet}$ , RO $^{\bullet}$  etc.) family (Prinn, 2003; Ehhalt, 1987; Khan et al., 2018). Among 12 them, OH• is considered as the most important oxidant in the troposphere (Lelieveld et al., 2002, 2016). Although OH• is the 13 most studied radical in the atmosphere, there are still open questions regarding its sources in the atmosphere (Heald and Kroll, 14 2021; Yang et al., 2024). For a long time, it was believed that OH radicals are mainly formed in daytime via photolysis of 15 tropospheric ozone (O<sub>3</sub>), and nitrous acid (HONO) (Calvert et al., 1994; Alicke et al., 2003; Griffith et al., 2016; Aumont et al., 16 2003). But now, with various on-field measurements (Geyer et al., 2003; Ren et al., 2003; Emmerson and Carslaw, 2009), it 17 is well established that OH radicals are also present at night in sufficient amounts. In fact, average nighttime concentration of 18  $OH^{\bullet}$  ( $\sim 2.6 \times 10^5$  molecule cm<sup>-3</sup>) is only one order of magnitude lower than its average daytime concentration ( $\sim 1.9 \times 10^6$ molecule cm $^{-3}$ ) (Emmerson and Carslaw, 2009). As the lifetime of OH $^{\bullet}$  is only  $\sim 1$  second, this much concentration of 20 21 OH• during night indicates its in situ generation via non-photolytic sources. The major non-photolytic source of OH• is the recycling of HO<sup>o</sup> radicals (Whalley et al., 2011; Stone et al., 2012; Hofzumahaus et al., 2009; Smith et al., 2006; Hens et al., 22 23 2013). Specifically, during the daytime, the primary reaction contributing to this recycling process is  $NO^{\bullet} + HO_{\bullet}^{\bullet}$ , whereas at night, the key reaction is NO<sub>3</sub> + HO<sub>2</sub> (Hall et al., 1988; Mellouki et al., 1988, 1993; Rai and Kumar, 2024). However, 24 25 compared to photolytic sources, non-photolytic sources of OH\* remain less understood in atmospheric chemistry (Brown and Stutz, 2012; Emmerson and Carslaw, 2009). This is evidenced by the fact that, in the atmosphere with a high concentration 26 of volatile organic compounds (VOCs), atmospheric models consistently under-predict the concentration of OH• compared to





the observed value (Emmerson and Carslaw, 2009; Stone et al., 2012). This discrepancy is especially pronounced in winter 28 (Harrison et al., 2006; Heard et al., 2004; Slater et al., 2020) and indoor environments (Østerstrøm et al., 2025; Gomez Alvarez 29 et al., 2013; Reidy et al., 2023), where light plays a minimal role. In addition, the discrepancy between measured and observed 30 31 value of OH• was also found to depend upon NO<sub>X</sub> concentration. Both under low NO<sub>X</sub> (Carslaw et al., 2001; Tan et al., 2001; Lelieveld et al., 2008; Tan et al., 2017) as well as high  $NO_X$  (above 6 ppbv) (Slater et al., 2020), the discrepancy was found to 32 be quite significant. As the primary recycling of  $HO_2^{\bullet}$  to  $OH^{\bullet}$  occurs via  $NO_X$ , the under-prediction of  $OH^{\bullet}$  by models under 33 low  $NO_X$  conditions suggests either the presence of another route for recycling or some new non-photolytic source of  $OH^{\bullet}$ . 34 This hypothesis is further strengthened by a few combined experimental and modelling studies. For example, Lu et al.(Lu 35 et al., 2012) have to introduce an artificial source of  $OH^{\bullet} \leftrightarrow HO_{2}^{\bullet}$  inter-conversion  $(RO_{2}^{\bullet} + X \longrightarrow HO_{2}^{\bullet}, HO_{2}^{\bullet} + X \longrightarrow OH^{\bullet})$  in 36 their atmospheric model to match the experimental concentration profile. In an another study, to match the experimental OH 37 concentration with models, Whalley et al. (Whalley et al., 2011) increased the concentration of VOCs in their model. Although 38 their computed OH<sup>•</sup> concentration becomes closer to experimental value, the mismatch between observed and measured con-39 40 centration of HO<sup>6</sup> becomes worse. There have been various attempts to identify the missing source of OH<sup>6</sup> in the atmosphere (Paulot et al., 2009; Peeters et al., 2014; Sander et al., 2019). For example, Peeters et al. (Peeters et al., 2009; Peeters and 41 42 Mu'ller, 2010; Peeters et al., 2014) suggested that the oxidation of isoprene can regenerate  $HO_X$  radicals in the presence of light via isoprene-peroxy radical interconversion and isomerisation pathways (Leuven Isoprene Mechanism (LIM)). Although 43 the introduction of LIM into chemical models were found to improve the value of modelled OH<sup>•</sup> concentration, the modelled 45 values still remain under-predicted (Crounse et al., 2011; Teng et al., 2017; Berndt et al., 2019; Novelli et al., 2020; J. Medeiros 46 et al., 2022). Particularly, the LIM is more effective in regions where biogenic volatile organic compounds (BVOCs) dominate and  $NO_X$  concentration is ultra low, e.g. rain forest regions (Whalley et al., 2011; Feiner et al., 2016; Lew et al., 2020). In 47 contrast, in regions where sufficient anthropogenic sources of VOCs are present, e.g. in polluted areas, LIM is not effective. 48 49 In addition, LIM is not fundamentally a HO<sup>o</sup><sub>2</sub> to OH<sup>o</sup> interconversion process, rather it is the recycling of VOCs to OH<sup>o</sup>. In a recent study, Yang et al. (Yang et al., 2024) suggested that aldehyde could be an additional source of OH. Authors proposed 50 that the autoxidation of carbonyl organic peroxy radicals (R(CO)O<sub>2</sub>) derived from higher aldehydes, can produce OH• through 51 photolysis (RAM mechanism). Though RAM mechanism efficiently predicts  $OH^{\bullet}$  production at low  $NO_X$  concentrations, it 52 still under-predicts the same at high  $NO_X$  concentrations. Interestingly, when both LIM and RAM are incorporated into a base 53 model in the presence of moderate concentration of  $NO_X$ ,  $OH^{\bullet}$  concentration improves significantly, but the discrepancy in the 54 modelled and observed HO<sup>o</sup> remains unresolved. It is also worth mentioning that photolysis is an important part of both, LIM 55 and RAM, and hence, both of these mechanism do not offer any help in improving the model OH\* concentration in nocturnal 56 57 environment. Furthermore, both LIM and RAM are also not directly involved in recycling of HO<sub>2</sub> to OH<sup>•</sup>. The discrepancy in the model occurs during both day and night (Faloona et al., 2001; Hens et al., 2013; Geyer et al., 2003), and is associated with 58 HO<sub>2</sub> to OH conversion (Whalley et al., 2011; Hofzumahaus et al., 2009). In light of these studies, we believe that the puzzle 59 of missing  $OH^{\bullet}$  source is very much alive and the key to this puzzle may be a non-photolytic source capable of  $HO_2^{\bullet} \leftrightarrow OH^{\bullet}$ 60 61 recycling.

In the present work, we are proposing reaction of Criegee intermediate with HONO as a source of OH<sup>•</sup>. Criegee Intermediates





(CIs) are formed during the ozonolysis of alkenes (Criegee, 1975; Johnson and Marston, 2008; Taatjes, 2017). In fact, alkene 63 ozonolysis is a highly exothermic reaction produces energized CIs. Some of the energized CIs readily convert into OH• via 64 unimolecular decomposition, while the remaining CIs get collisionally stabilized (sCI) (Horie and Moortgat, 1991; Donahue 65 66 et al., 2011; Novelli et al., 2014; Alam et al., 2011). sCIs can undergo either a thermal unimolecular dissociation or a bimolecular reaction. Depending upon concentration of the co-reactant and rate constant of such bimolecular reaction, the bimolecular 67 reaction paths can be the main sink of sCI (Osborn and Taatjes, 2015; Lin et al., 2015; Sheps et al., 2014; Vereecken and 68 Francisco, 2012). There are several studies in the literature that suggest CI reacts rapidly with the trace gases present in the 69 atmosphere (Cox et al., 2020; Mallick and Kumar, 2020; Vereecken et al., 2015). In this work, we are suggesting HONO as 70 a new partner for the bimolecular reaction of Criegee intermediates as a possible source of OH $^{\bullet}$ . The concentration of CI ( $\sim$ 71  $10^4 - 10^5$  molecule cm<sup>-3</sup>) in the atmosphere is comparable with Cl $^{\bullet}$  ( $\sim 5.0 \times 10^4 - 3.0 \times 10^5$  molecule cm $^{-3}$ ) and OH $^{\bullet}$  ( $\sim$ 72  $1.0 \times 10^5 - 4.0 \times 10^6$  molecule cm $^{-3}$ ) (Khan et al., 2018; Novelli et al., 2017). Similarly, nitrous acid (HONO) is also an im-73 portant trace gas present in the nighttime atmosphere in a considerable amount (Li et al., 2021; Song et al., 2023). The average 74 concentration of HONO is  $\sim 8.9 \times 10^{10}$  molecule cm<sup>-3</sup>, which can reach as high as  $\sim 6.9 \times 10^{11}$  molecule cm<sup>-3</sup> during the 75 fog event (Pawar et al., 2024). Although a general wisdom about HONO is, its concentration builds up in nighttime, and in 76 77 daytime, it decomposes via photolysis to give OH<sup>•</sup>, HONO itself is a highly reactive molecule and can participate in various bimolecular chemical reactions during night (Anglada and Sole, 2017; Lu et al., 2000; Wallington and Japar, 1989). Moreover, 78 79 in indoor environments, high concentrations of OH• have been found to strongly correlate with high concentrations of HONO (Gomez Alvarez et al., 2013). It is important to mention that, the reaction of HONO with the simple Criegee intermediate 80 (CH<sub>2</sub>OO) has already been investigated theoretically (Kumar et al., 2022). In that investigation, the major product was pre-81 dicted to be hydroperoxymethyl nitrite (HPMN). We will show in the present work that the main product of this reaction is 82 OH• and this path is the dominant path of the title reaction. 83

# 84 2 Methodology

There are two parts of electronic structure theory; optimization and subsequent single-point energy calculations. The criteria 85 behind choosing a method for optimization is; it should be computationally not very demanding and at the same time, it 86 should accurately predict the geometries and frequencies of the species involved in the reaction. Based on these criteria, all 87 the geometries have been optimized using M06-2X functional in conjuction with aug-cc-pVTZ basis set using Gaussian16 88 software package (Frisch et al., 2016). We have compared the geometrical parameters of the isolated species obtained at M06-89 2X/aug-cc-pVTZ level of theory with the experimental (Johnson III, 2013; Ruscic et al., 2004) values available in the literature 90 in Figure S1 of the ESI. It is evident from Figure S1 that the maximum deviation in bond lengths at M06-2X/aug-cc-pVTZ level of theory from the experiment was only  $\sim 0.04$  Å, whereas the maximum deviation in bond angles from the experiment was 92  $\sim 1^{\circ}$ . It clearly suggests that M06-2X/aug-cc-pVTZ level of theory is providing accurate geometries of the isolated species. 93 In addition, we have also compared the frequencies of the isolated species obtained at M06-2X/aug-cc-pVTZ level of theory 94 with the experimental values in Table S2 of the ESI. The maximum deviation in frequency from experiment was  $\sim 250 \text{ cm}^{-1}$ .



100

103



Therefore, we believe that M06-2X/aug-cc-pVTZ level of theory is appropriate for optimization and frequency calculations. 96

This conclusion is also consistent with the previous work (Kumar et al., 2022) where M06-2X/aug-cc-pVTZ level of theory 97

was found to be adequate for the title reaction. For the second part, we carried out single-point energy calculations for the 98

99 optimized geometries at CCSD(T) level of theory in complete basis set limit (CBS). To estimate energies at CCSD(T)/CBS

level of theory, first, we calculated the single point energies at CCSD(T)/aug-cc-pVDZ, and CCSD(T)/aug-cc-pVTZ level of

theory, and then extrapolated these energies to corresponding CBS limit using the method of Varandas and Pansini (Varandas 101

and Pansini, 2014; Pansini et al., 2016) (see ESI for the details). 102

#### 3 Results and discussion

In the present work, we have investigated the reactions of Criegee intermediates (CIs) with nitrous acid (HONO). It is known 104

that the reactivity of CI is greatly influenced by the substitution group present on carbon center of the CI. Therefore, to 105

106 account for it, we have studied two types of CIs; the simplest Criegee intermediate (CH<sub>2</sub>OO) and the dimethyl-substituted

Criegee intermediate ((CH<sub>3</sub>)<sub>2</sub>COO). Another motivation for choosing (CH<sub>3</sub>)<sub>2</sub>COO comes from the fact that in contrast to 107

simple Criegee which is formed only from the ozonolysis of ethene, the dimethyl-substituted Criegee intermediate can be 108

generated from the ozonolysis of many highly abundant alkenes, such as terpenes and mycrene, and hence, the concentration 109

of (CH<sub>3</sub>)<sub>2</sub>COO is significantly higher in the atmosphere. In this section, we will first discuss the energetics and kinetics of 110

CH<sub>2</sub>OO + HONO reaction, followed by (CH<sub>3</sub>)<sub>2</sub>COO + HONO reaction. 111

The potential energy surface for CH<sub>2</sub>OO + HONO reaction is depicted in Figure 1. It is evident from Figure 1 that reaction 112

occurs in two steps; in the first step, CH<sub>2</sub>OO interacts with H atom of HONO via hydrogen bonding and forms a stable reactant-113

complex (RC1), which is  $\sim 10.1$  kcal mol<sup>-1</sup> stable than isolated reactants. In the next step, RC undergoes a unimolecular 114

transformation to form final products, i.e., CH<sub>2</sub>O, OH<sup>•</sup>, and NO<sub>2</sub>. This happens via a transition-state (TS1) that is effectively 115

 $\sim 8.0$  kcal mol<sup>-1</sup> below the isolated reactants. It suggests that the formation of OH $^{\bullet}$  via CH<sub>2</sub>OO + HONO reaction is a 116

barrierless process. The overall reaction was found to be exothermic by  $\sim 17.3$  kcal mol<sup>-1</sup> that lies close to the experimental 117

value of  $\sim 16.9$  kcal mol<sup>-1</sup> (Ruscic et al., 2004), again confirming the adequacy of the methodology used. 118

Energetics calculations shed light only on enthalpic requirement of the reaction, for a barrierless process, entropy is an equally 119

important factor. Therefore, to account for both, enthalpy and entropy, we have estimated the rate constant for CH<sub>2</sub>OO + 120

HONO reaction within a temperature range of 213–320 K. The mechanism of CH<sub>2</sub>OO + HONO reaction can be represented 121

by following reaction: 122

123 
$$CH_2OO + HONO \xrightarrow{k_f} RC1 \xrightarrow{k_{uni}} CH_2O + OH^{\bullet} + NO_2$$
 (R1)

In reaction R1, the bimolecular rate constant  $(k_{bi})$  can be calculated using following equation: 124

$$\mathbf{k}_{bi} = \mathbf{k}_f \times \gamma$$

Here,  $k_f$  represents the rate of the formation of RC1 from the isolated reactants (capture rate) which is estimated using 126

KTOOLS code as implemented in MultiWell suite of programs (Barker et al., 2021).  $\gamma$  is the product branching ratio for



131

132



RC1 computed from the relative yields of reactants ( $\eta_{reac}$ ) and products ( $\eta_{prod}$ ) starting from the RC1, which can be defined as follows:

Here,  $\gamma$  was computed using a master equation approach as implemented in MultiWell suite of programs (Barker et al.,

2021) (see ESI for the details). The computed bimolecular rate constant values ( $k_{bi}^{CH_2OO}$ ) for CH<sub>2</sub>OO + HONO reaction in the

$$\gamma = \frac{\eta_{prod}}{\eta_{reac} + \eta_{prod}}$$

temperature range 213–320 K are given in Table 1. It is evident from Table 1 that the values of  $\mathbf{k}_{hi}^{CH_2OO}$  do not change much 133 with temperature, a typical character of a barrierless process. For example, at 213 K, values of  $k_{bi}^{CH_2OO}$  is  $3.9 \times 10^{-12}$  cm<sup>3</sup> 134  $molecule^{-1} sec^{-1}$  which becomes  $\sim 3.1 \times 10^{-12}$  cm<sup>3</sup>  $molecule^{-1} sec^{-1}$  at 320 K. 135 Figure 2 depicts the potential energy surface of (CH<sub>3</sub>)<sub>2</sub>COO + HONO reaction. It is evident from Figure 2 that (CH<sub>3</sub>)<sub>2</sub>COO 136 + HONO reaction also proceeds in two steps; in the first step, (CH<sub>3</sub>)<sub>2</sub>COO associates with HONO to form a stable reactant-137 complex (RC2) that is  $\sim 14.2$  kcal mol<sup>-1</sup> more stable than isolated reactants. Finally, RC transforms into isolated products, 138 i.e.,  $(CH_3)_2CO$ ,  $OH^{\bullet}$ , and  $NO_2$ . This transformation occurs through a transition state that lies  $\sim 10.1$  kcal mol<sup>-1</sup> below the 139 isolated reactants, making the overall reaction barrierless. 140 Using the energetics, we have also computed the rate constant for (CH<sub>3</sub>)<sub>2</sub>COO + HONO reaction employing master equation 141 in the same 213–320 K temperature range. The calculated bimolecular rate constants  $(k_{bi}^{(CH_3)_2COO})$  are listed in Table 1. It is 142 evident from Table 1 that similar to CH<sub>2</sub>OO + HONO reaction, here also the values of  $k_{bi}^{(CH_3)_2COO}$  remain almost constant 143 within whole range of temperature. But the bimolecular rate constant of  $(CH_3)_2COO + HONO$  reaction becomes  $\sim$  one order 144 of magnitude higher compared to the same for CH<sub>2</sub>COO + HONO reaction at all temperatures considered in the present work. For example, at 298 K, the value of  $k_{bi}^{(CH_3)_2COO}$  is  $\sim 3.5 \times 10^{-11}$  cm<sup>3</sup> molecule<sup>-1</sup> sec<sup>-1</sup>, whereas the value of  $k_{bi}^{CH_2OO}$  is only 146  $\sim 3.4 \times 10^{-12}~{\rm cm}^3~{\rm molecule}^{-1}~{\rm sec}^{-1}$ . To understand the difference in the rate values of the two reactions, we have provided 147 the components of the bimolecular rate constants (capture rates and  $\gamma$  values) in Table S3 of the ESI. One can see from Table 148 S3 that the capture rates of both the reactions are almost same, while the  $\gamma$  values are higher for (CH<sub>3</sub>)<sub>2</sub>COO + HONO reaction 149 150 compared to CH<sub>2</sub>COO + HONO. Therefore, it is the  $\gamma$  that increases the overall bimolecular rate of (CH<sub>3</sub>)<sub>2</sub>COO + HONO reaction. As mentioned above,  $\gamma$  is the product branching ratio starting from a reactant complex, i.e., it indicates the extent to 151 which the reactant complex will proceed forward or backward. This further depends on the forward and backward Gibbs free 152 153 energy barriers of the reactant complex. The Gibbs free energy profile at 298 K is shown in Figure S2 of the ESI. It is evident from Figure S2 that due to the higher stabilization of RC2, its reverse free energy barrier is high ( $\sim 2.9 \text{ kcal mol}^{-1}$ ), while 154 the same is very low for RC1 ( $\sim$  -1.3 kcal mol<sup>-1</sup>). Consequently,  $\gamma_{reac}$  is much lower than  $\gamma_{prod}$  of RC2, leading to a higher 155 value of  $\gamma$  for (CH<sub>3</sub>)<sub>2</sub>COO + HONO reaction. 156

## 4 Atmospheric implications

157

After estimating the energetics and kinetics of title reaction, it is important to discuss the impact of title reaction in the atmosphere critically depends on how it competes with other known



194



sinks of Criegee intermediate, i.e., H<sub>2</sub>O, (H<sub>2</sub>O)<sub>2</sub>, NO<sub>2</sub>, NO, CO, and SO<sub>2</sub>. The efficiency of a chemical reaction in the atmo-160 sphere depends upon two factors; rate of reaction and concentration of co-reactants. The effective rate constant  $(k_{eff})$  captures 161 both of these factors as it is defined as the multiplication of bimolecular rate and concentration of co-reactants. Therefore, 162 163 we have used  $k_{eff}$  to compare the effectiveness of title reaction compared to other sinks of Criegee intermediates. A list of effective rates for the reaction of CI with H<sub>2</sub>O, (H<sub>2</sub>O)<sub>2</sub>, NO<sub>2</sub>, NO, CO, and SO<sub>2</sub> at 298 K are provided in Table S4 of the ESI. 164 165 To compute  $k_{eff}$ , the average concentrations of all the sinks have been taken from polluted urban environments. The corresponding rate coefficients of all the sinks are taken from experimental measurements. One can see from Table S4, the effective 166 rate coefficients ( $k_{eff}$ ) of CO, NO, and NO<sub>2</sub> are lower compared to those of SO<sub>2</sub>, H<sub>2</sub>O, and (H<sub>2</sub>O)<sub>2</sub>. For example,  $k_{eff}$  for the 167 reaction of CI with SO<sub>2</sub> is 3.35 sec<sup>-1</sup>, while that for NO<sub>2</sub> is only 0.9 sec<sup>-1</sup>. Therefore, in the present work, we have focused 168 our attention on a detailed comparison of the title reaction with SO<sub>2</sub>, H<sub>2</sub>O, and (H<sub>2</sub>O)<sub>2</sub>. As far as the unimolecular decomposi-169 tion pathway of Criegee intermediates is concerned, it is more effective with energized and bigger Criegee species, which are 170 formed during ozonolysis of alkenes. The stabilized Criegee such as unsubstituted and disubstituted Criegee intermediates can 171 dissociate via bimolecular reactions with radicals, depending upon their concentration in the atmosphere. 172 173 HONO concentrations are found to be significantly higher in polluted urban areas, such as megacities. Therefore, we expect 174 HONO to play a more effective role as a sink for Criegee intermediates in such regions, and hence, we have taken the representative concentrations of HONO and SO<sub>2</sub> in urban areas for a primary comparison. The concentration of water varies greatly in 175 the atmosphere depending upon saturation vapour pressure and relative humidity (RH) (Anglada et al., 2013; Rai and Kumar, 176 177 2025). Therefore, in the case of H<sub>2</sub>O and (H<sub>2</sub>O)<sub>2</sub>, we have taken two concentrations; one calculated at 20% RH, and the other calculated at 100% RH. The former serves as lower limits of H<sub>2</sub>O and (H<sub>2</sub>O)<sub>2</sub> concentrations, whereas the latter serves as the 178 upper limits of  $H_2O$  and  $(H_2O)_2$  concentrations. 179 180 In Figure 3, we have compared the  $k_{eff}$  of  $CH_2OO + HONO$  with the  $k_{eff}$  of  $CH_2OO + H_2O/(H_2O)_2/SO_2$  reactions. Figure 3 shows, at 100% RH,  $k_{eff}$  of CH<sub>2</sub>OO + (H<sub>2</sub>OO<sub>2</sub> is the dominant reaction across the entire temperature range (213–320 K) (Lin 181 et al., 2016). At 20% RH, k<sub>eff</sub> for CH<sub>2</sub>OO + (H<sub>2</sub>O)<sub>2</sub> and CH<sub>2</sub>OO + H<sub>2</sub>O remain dominant at higher temperatures, specif-182 ically within 235–320 K and 245–320 K, respectively. However, at lower temperatures,  $k_{eff}$  of CH<sub>2</sub>OO + HONO becomes 183 dominant, surpassing both, CH<sub>2</sub>OO + (H<sub>2</sub>O)<sub>2</sub> and CH<sub>2</sub>OO + H<sub>2</sub>O in the range of 213–235 K and 213–245 K, respectively. 184 As far as  $CH_2OO + SO_2$  reaction is concerned (Onel et al., 2021), its  $k_{eff}$  values are  $\sim$  one order of magnitude higher than 185 that of CH<sub>2</sub>OO + HONO reaction within the whole temperature range, indicating that CH<sub>2</sub>OO + HONO reaction is a minor 186 contributor compared to  $CH_2OO + SO_2$ . 187 Similarly, we have compared our dimethyl substituted Criegee reaction ((CH<sub>3</sub>)<sub>2</sub>COO + HONO) with other known bimolec-188 189 ular reactions of  $(CH_3)_2COO$ . Here also we have computed  $k_{eff}$  for the comparison (see Figure 4). The rate constants of  $(CH_3)_2COO + SO_2$  reaction (Smith et al., 2016) is known in the range of 283–303 K, and hence, we have compared its  $k_{eff}$  in 190 191 this temperature range with dimethyl substituted (CH<sub>3</sub>)<sub>2</sub>COO + HONO reaction. Figure 4 shows that unlike CH<sub>2</sub>OO + HONO reaction, here  $k_{eff}$  of  $(CH_3)_2COO + HONO$  is one order of magnitude higher than the same for  $(CH_3)_2COO + SO_2$  reaction 192 within 283-303 K. In addition, it is worth mentioning that under certain atmospheric conditions, concentration of HONO can 193

be quite high compared to SO<sub>2</sub>. For example, during fog events, it is well known that concentration of SO<sub>2</sub> drops significantly



195



Criegee intermediates in fog-like environments. In addition, as SO<sub>2</sub> mainly comes from human activities, its concentrations 196 are high in polluted areas and become quite very low in tropical forests and rural areas. In fact, its concentrations fall below 197 198 detection limits in tropical forest regions (Vereecken et al., 2012). In contrast, although HONO concentration is also high in polluted regions compared to a clean environment, due to the various in situ sources, HONO is present in reasonable amounts 199 even in tropical forest areas (Zhang et al., 2012). Therefore, in this region also, HONO is a more effective sink of CI com-200 pared to SO<sub>2</sub>. Moreover, CI + HONO reaction is a hydrogen atom transfer (HAT) process, and hence, the presence of water 201 can effectively catalyze this reaction (Buszek et al., 2012; Viegas and Varandas, 2012; Rai and Kumar, 2025). In contrast, the 202 presence of water, particularly droplets and aerosols, can act as a sink for SO<sub>2</sub> (Zhang et al., 2013), and hence, in the presence 203 of water, Criegee + SO<sub>2</sub> reaction should be less important compared to CI + HONO reaction. After establishing that compared 204 to SO<sub>2</sub>, HONO is a more effective sink for (CH<sub>3</sub>)<sub>2</sub>COO under most of the conditions, at last, it is important to compare it 205 with (CH<sub>3</sub>)<sub>2</sub>COO + H<sub>2</sub>O/(H<sub>2</sub>O)<sub>2</sub> reactions (Vereecken et al., 2017). It is evident from Figure 4 that at 100% RH, k<sub>eff</sub> of 206  $(CH_3)_2COO + HONO$  can dominate over  $k_{eff}$  of  $(CH_3)_2COO + H_2O$  and  $(CH_3)_2COO + (H_2O)_2$  for a relatively wider range 207 of temperatures. For example, the dominant temperature range of (CH<sub>3</sub>)<sub>2</sub>COO + HONO is, 213–275 K for (CH<sub>3</sub>)<sub>2</sub>COO + 208 209  $(H_2O)_2$  and 213–290 K for  $(CH_3)_2COO + H_2O$ . At 20% RH,  $k_{eff}$  of  $(CH_3)_2COO + HONO$  becomes dominant over  $k_{eff}$  of both, (CH<sub>3</sub>)<sub>2</sub>COO + H<sub>2</sub>O and (CH<sub>3</sub>)<sub>2</sub>COO + (H<sub>2</sub>O)<sub>2</sub> in almost whole temperature range (213–310 K). For example, at 298 210 K,  $k_{eff}$  of  $(CH_3)_2COO + HONO$  is  $\sim 3.1 \text{ sec}^{-1}$ , which is three times and four times higher than the same for  $(CH_3)_2COO$ 211 + H<sub>2</sub>O and (CH<sub>3</sub>)<sub>2</sub>COO + (H<sub>2</sub>O)<sub>2</sub>, respectively. This suggests that the major sink of substituted CI can be its reaction with 212 HONO in the atmosphere even in the presence of high humidity and  $SO_2$ . 213 Finally, it is important to assess the extent to which the title reaction can contribute in resolving the puzzle of mismatch be-214 tween measured and modelled OH\*/HO\* concentrations. It is important to mention that during daytime, HONO undergoes 215 rapid photolysis; therefore, its concentration is higher in the absence of light, e.g. at night, indoors, in winter, etc. For example, 216 the photolysis rate of HONO is known to be  $\sim 10^{-3}~{\rm sec}^{-1}$ , which is several orders of magnitude higher than the effective rate 217 constant of its reaction with Criegee intermediates ( $\sim 10^{-7} - 10^{-6}~\text{sec}^{-1}$ , computed using maximum Criegee concentration 218 of  $\sim 10^5$  molecule cm<sup>-3</sup>) (Shabin et al., 2023). Therefore, during the peak of daytime, title reaction does not contribute much 219 220 to OH<sup>•</sup> production; rather, it can play a key role in nocturnal atmospheric chemistry, specifically at times when both, concentrations of HONO and CI are high, and, at the same time, the presence of light is minimal. To understand the efficiency of the 221 title reaction in affecting  $OH^{\bullet}$  concentration in a nocturnal environment, we can compare it with  $NO_3^{\bullet} + HO_2^{\bullet}$  reaction, which 222 is a well-known source of OH<sup>•</sup> at nighttime. The rate constants for both the reactions are similar. For example, at 298 K, the 223 rate value for CH<sub>2</sub>OO + HONO is  $\sim 3.35 \times 10^{-12}$  cm<sup>3</sup> molecule<sup>-1</sup> sec<sup>-1</sup>, which is almost identical to the rate value (Rai and 224 Kumar, 2024) for  $NO_3^{\bullet}$  +  $HO_2^{\bullet}$ , i.e.,  $\sim 3.36 \times 10^{-12}$  cm<sup>3</sup> molecule<sup>-1</sup> sec<sup>-1</sup>. In the atmosphere, average concentration of both 225  $NO_3^{\bullet}$  and  $HO_2^{\bullet}$  are  $\sim 10^8$  molecule cm<sup>-3</sup>(Bottorff et al., 2023; Brown and Stutz, 2012), thus combined concentration turns out 226 to be  $\sim 10^{16}$  molecule<sup>2</sup> cm<sup>-6</sup>. Similarly, the combined concentration will be  $\sim 10^{15}$  molecule<sup>2</sup> cm<sup>-6</sup> for CH<sub>2</sub>OO + HONO 227 under high concentrations of CI ( $\sim 10^5$  molecule cm<sup>-3</sup>)(Khan et al., 2018) and HONO ( $\sim 10^{10}$  molecule cm<sup>-3</sup>)(Pawar et al., 228 2024). It suggests that CH<sub>2</sub>OO + HONO reaction may be somewhat slower in producing OH•. However, since the rate of 229

(Zhang et al., 2013) while concentration of HONO increases (Pawar et al., 2024), making HONO a potentially major sink of



238



(CH<sub>3</sub>)<sub>2</sub>COO + HONO reaction is one order of magnitude higher compared to NO<sub>3</sub> + HO<sub>2</sub>, we believe both NO<sub>3</sub> + HO<sub>2</sub> and 230 title reactions should be of similar importance as far as the production of nighttime OH• is concerned. In other words, title 231 reaction has the potential to serve as a significant contributor to OH• production in nighttime atmospheric chemistry. 232 Another factor worth noting is, besides OH<sup>•</sup>, the title reaction produces HCHO/(CH<sub>3</sub>)<sub>2</sub>CO, and NO<sup>•</sup><sub>2</sub> as products. It is well 233 known that both HCHO/(CH<sub>3</sub>)<sub>2</sub>CO (Gao et al., 2024; Long et al., 2022; Hermans et al., 2004) and NO<sub>2</sub> (Christensen et al., 234 2004) can act as sinks for HO<sub>2</sub> radicals (corresponding reactions are listed in the box below). It suggests that title reaction has 235 the potential for recycling of  $HO_2^{\bullet} \leftrightarrow OH^{\bullet}$  process. To illustrate the ability of title reaction in recycling  $HO_2^{\bullet} \leftrightarrow OH^{\bullet}$  process, 236 we have developed a kinetic model consisting of the following reactions (see ESI for the details): 237

$$\begin{array}{c} \hline \\ CH_2OO/(CH_3)_2COO + HONO & \frac{k_{CH_2OO}/}{k_{(CH_3)_2COO}} OH^{\bullet} + HCHO/(CH_3)_2CO + NO_2^{\bullet} \\ \\ HCHO/(CH_3)_2CO + HO_2^{\bullet} & \frac{k_{HCHO}/}{k_{(CH_3)_2CO}} & HOCH_2OO/(CH_3)_2C(OH)OO \\ \\ NO_2^{\bullet} + HO_2^{\bullet} & \xrightarrow{k_{NO_2^{\bullet}}} & HO_2NO_2 \\ \hline \end{array}$$

This model requires two key components: first, the rate coefficients of the relevant reactions, which have been taken from 239 the recommended literature values (Gao et al., 2024; Hermans et al., 2004; Long et al., 2022; Christensen et al., 2004), and 240 second, a list of realistic initial concentrations of the reactive species involved in  $HO_2^{\bullet} \leftrightarrow OH^{\bullet}$  recycling process (Table S5 241 of the ESI). We first tracked the change in concentration of OH<sup>•</sup> and HO<sup>•</sup> using the first kinetic model consisting of CH<sub>2</sub>OO 242 243 + HONO reaction, followed by second model consisting of (CH<sub>3</sub>)<sub>2</sub>COO + HONO reaction. Initial concentrations of relevant species (HCHO, HONO, (CH<sub>3</sub>)<sub>2</sub>CO, and HO<sub>2</sub>) were chosen based on literature values representing polluted urban conditions 244 (Vereecken et al., 2012; Pawar et al., 2024). Although the average concentration of OH $^{\bullet}$  can vary within  $\sim 10^4$ – $10^6$  molecules 245  ${\rm cm}^{-3}$  in the atmosphere, we have used a modelled value of it in the present work. In CH<sub>2</sub>OO + HONO reaction model, 246 the initial OH $^{\bullet}$  concentration was set to  $\sim 10^4$  molecules cm $^{-3}$ , while in (CH $_3$ ) $_2$ COO + HONO model, it was set to  $\sim 10^5$ 247 molecules cm<sup>-3</sup>. This difference was chosen based on how much OH each reaction is expected to produce when no in situ 248 reactions are taking place from the byproducts of the title reaction. Since (CH<sub>3</sub>)<sub>2</sub>COO + HONO reaction can generate more 249 OH, starting with a higher initial concentration helps one observe a noticeable change in OH• levels during the simulation. 250 This makes it easier to observe and compare the effect of OH<sup>•</sup> production between the two reactions. It is important to mention 251 that the maximum concentration of  $OH^{\bullet}$  can be taken as  $\sim 10^5$  molecules cm<sup>-3</sup> in the kinetic model. This is because the 252 production of OH $^{\bullet}$  is limited by the available concentration of CI which can be as high as  $\sim 10^5$  molecules cm $^{-3}$ . Therefore, 253 taking  $OH^{\bullet}$  concentration more than  $\sim 10^5$  molecules cm<sup>-3</sup> would produce no effect on the concentration of  $OH^{\bullet}$ . This also 254 reveals the fact that the title reaction is capable of producing OH• in regions where the concentration of OH• is already low. 255 Similarly, the concentration of NO<sub>2</sub> can vary within  $\sim 10^{10}$ – $10^{12}$  molecules cm<sup>-3</sup> in polluted urban regions. However, in the 256 present model, we have kept it at  $\sim 10^{10}$  molecules cm<sup>-3</sup> in order to observe a clear numerical change in the values of HO<sub>2</sub>. 257 Taking a high concentration of  $NO_2$  ( $\sim 10^{12}$  molecules cm<sup>-3</sup>) would drastically consume  $HO_2^{\bullet}$ , and a gradual change would 258





259 not be observed.

We have divided the simulation results into two parts; first we will discuss  $CH_2OO + HONO$  reaction followed by  $(CH_3)_2COO$ 260 + HONO. The model results have been shown in Figure 5. It is evident from Figure 5 that CH<sub>2</sub>OO + HONO reaction increases 261 OH• concentration while simultaneously reducing HO• concentration. Quantitatively, this reaction increases OH• production 262 by five times its initial value while decreasing HO<sub>2</sub> production by more than one order of magnitude. Furthermore, when 263 we consider dimethyl-substituted Criegee intermediate reaction ((CH<sub>3</sub>)<sub>2</sub>COO + HONO), OH• production has been found to 264 increase by only two times compared to its initial concentration, while HO<sup>o</sup><sub>2</sub> production again decreases by the same one order 265 of magnitude (Figure 5). The difference in OH• production can be attributed to the fact that, in case of (CH<sub>3</sub>)<sub>2</sub>COO + HONO, 266 the initial OH $^{\bullet}$  concentration was taken to be  $\sim 10^5$  molecules cm $^{-3}$  compared to  $\sim 10^4$  molecules cm $^{-3}$  in case of CH<sub>2</sub>OO 267 + HONO. This further strengthens the fact that the effect of title reaction on OH• production will be more pronounced in 268 the conditions where OH• concentration is lower in the atmosphere, e.g., at night. The overall simulation results suggest that 269 incorporating title reaction into atmospheric models can improve their accuracy in predicting OH• and HO• concentrations. 270 However, a more realistic impact of the title reaction on the budget of both OH• and HO•, requires a more complete modeling. 271 In order to do so, one needs accurate estimation of the rate constants for the reaction of HONO with various important Criegee 272 273 intermediates. For bigger Criegee intermediates, computation will be more costly and require a separate study. In addition, being a HAT reaction, the effect of humidity on the title reaction is also important to build a complete model. 274

## 275 5 Conclusions

285 286

287

In this work, we studied the energetics and kinetics of bimolecular reaction of simple and dimethyl-substituted Criegee with 276 HONO using high-level electronic structure theory and chemical kinetics. Our quantum chemical calculations suggest that both 277 of the reactions are barrierless and kinetic calculations reveal that reaction of substituted Criegee with HONO is one order of 278 magnitude faster than simple Criegee + HONO reaction. By comparing it with other known sinks of CI, we have shown that 279 280 this reaction can serve as a major sink for Criegee intermediates in most of the atmospheric conditions, even in the presence of high humidity and SO<sub>2</sub>. In addition, we have also shown that title reaction can be one of the most important source of OH• in 281 nocturnal atmosphere. In addition, the products of CI + HONO reaction can be a sink for HO<sub>2</sub> radicals, and hence this reaction 282 is capable of  $HO_2^{\bullet} \leftrightarrow OH^{\bullet}$  recycling. Consequently, this reaction can be key in fulfilling the gap between the observed OH283 radicals and modelled values. At last, we look forward to the experimental verification of our results. 284

Author contributions. VJA: Conducted the investigation, Writing – original draft, Formal analysis, curated the data. PKR: Contributed to writing, reviewing, and editing the manuscript. PK: Provided supervision, resources, and methodology; conceptualized the study; acquired funding; and contributed to the review and editing of the manuscript.





288 Competing interests. The authors declare that they have no conflict of interest.

289 Acknowledgements. V.J.A. and P.K.R acknowledge MNIT Jaipur for financial assistance. P.K. acknowledges DST, Govt. of India, for the

290 financial support through the sanctioned project No. EEQ/2023/000351.





## 291 References

- 292 Alam, M. S., Camredon, M., Rickard, A. R., Carr, T., Wyche, K. P., Hornsby, K. E., Monks, P. S., and Bloss, W. J.: Total radical yields from
- tropospheric ethene ozonolysis, Phys. Chem. Chem. Phys., 13, 11 002–11 015, 2011.
- 294 Alicke, B., Geyer, A., Hofzumahaus, A., Holland, F., Konrad, S., Pätz, H., Schäfer, J., Stutz, J., Volz-Thomas, A., and Platt, U.: OH formation
- by HONO photolysis during the BERLIOZ experiment, J. Geophys. Res., 108, PHO-3, 2003.
- 296 Anderson, J. G.: Free Radicals in the Earth's Atmosphere: Their Measurement and Interpretation, Annu. Rev. Phys. Chem., 38, 489-520,
- 297 1987.
- 298 Anglada, J. M. and Sole, A.: The atmospheric oxidation of HONO by OH, Cl, and ClO radicals, J. Phys. Chem. A, 121, 9698–9707, 2017.
- 299 Anglada, J. M., Hoffman, G. J., Slipchenko, L. V., M. Costa, M., Ruiz-Lopez, M. F., and Francisco, J. S.: Atmospheric significance of water
- 300 clusters and ozone–water complexes, J. Phys. Chem. A, 117, 10381–10396, 2013.
- 301 Aumont, B., Chervier, F., and Laval, S.: Contribution of HONO sources to the NO<sub>X</sub>/HO<sub>X</sub>/O<sub>3</sub> chemistry in the polluted boundary layer,
- 302 Atmos. Environ., 37, 487–498, 2003.
- 303 Barker, J., Nguyen, T., Stanton, J., Aieta, C., Ceotto, M., Gabas, F., Kumar, T., Li, C., Lohr, L., Maranzana, A., et al.: MultiWell-2021 Software
- 304 Suite; J. R. Barker, University of Michigan, Ann Arbor, Michigan, USA, http://claspresearch.engin.umich.edu/multiwell/ (accessed march
- 305 5, 2025), 2021.
- 306 Berndt, T., Hyttinen, N., Herrmann, H., and Hansel, A.: First oxidation products from the reaction of hydroxyl radicals with isoprene for
- pristine environmental conditions, Commun. Chem., 2, 21, 2019.
- 308 Bottorff, B., Lew, M. M., Woo, Y., Rickly, P., Rollings, M. D., Deming, B., Anderson, D. C., Wood, E., Alwe, H. D., Millet, D. B., et al.: OH,
- 309 HO 2, and RO 2 radical chemistry in a rural forest environment: measurements, model comparisons, and evidence of a missing radical
- 310 sink, Atmos. Chem. Phys., 23, 10 287–10 311, 2023.
- 311 Brown, S. S. and Stutz, J.: Nighttime radical observations and chemistry, Chem. Soc. Rev., 41, 6405–6447, 2012.
- 312 Buszek, R. J., Barker, J. R., and Francisco, J. S.: Water effect on the OH + HCl reaction, J. Phys. Chem. A, 116, 4712–4719, 2012.
- 313 Calvert, J., Yarwood, G., and Dunker, A.: An evaluation of the mechanism of nitrous acid formation in the urban atmosphere, Res. Chem.
- 314 Intermed., 20, 463–502, 1994.
- 315 Carslaw, N., Creasey, D., Harrison, D., Heard, D., Hunter, M., Jacobs, P., Jenkin, M., Lee, J., Lewis, A., Pilling, M., et al.: OH and HO<sub>2</sub>
- radical chemistry in a forested region of north-western Greece, Atmos. Environ., 35, 4725–4737, 2001.
- 317 Christensen, L. E., Okumura, M., Sander, S. P., Friedl, R. R., Miller, C. E., and Sloan, J. J.: Measurements of the Rate Constant of HO<sub>2</sub> +
- 318 NO<sub>2</sub> + N<sub>2</sub>  $\longrightarrow$  HO<sub>2</sub>NO<sub>2</sub> + N<sub>2</sub> Using Near-Infrared Wavelength-Modulation Spectroscopy and UV- Visible Absorption Spectroscopy, J.
- 319 Phys. Chem. A, 108, 80-91, 2004.
- 320 Cox, R. A., Ammann, M., Crowley, J. N., Herrmann, H., Jenkin, M. E., McNeill, V. F., Mellouki, A., Troe, J., and Wallington, T. J.: Evaluated
- 321 kinetic and photochemical data for atmospheric chemistry: Volume VII–Criegee intermediates, Atmos. Chem. Phys., 20, 13 497–13 519,
- 322 2020.
- 323 Criegee, R.: Mechanism of ozonolysis, Angew. Chem. internat. Edit., 14, 745–752, 1975.
- 324 Crounse, J. D., Paulot, F., Kjaergaard, H. G., and Wennberg, P. O.: Peroxy radical isomerization in the oxidation of isoprene, Phys. Chem.
- 325 Chem. Phys., 13, 13 607–13 613, 2011.
- 326 Donahue, N. M., Drozd, G. T., Epstein, S. A., Presto, A. A., and Kroll, J. H.: Adventures in ozoneland: down the rabbit-hole, Phys. Chem.
- 327 Chem. Phys., 13, 10848–10857, 2011.





- 328 Ehhalt, D.: Free Radicals in the Atmosphere, Free Radic. Res. Commun., 3, 153–164, 1987.
- 329 Emmerson, K. and Carslaw, N.: Night-time radical chemistry during the TORCH campaign, Atmos. Environ., 43, 3220–3226, 2009.
- 330 Faloona, I., Tan, D., Brune, W., Hurst, J., Barket Jr, D., Couch, T. L., Shepson, P., Apel, E., Riemer, D., Thornberry, T., et al.: Nighttime
- observations of anomalously high levels of hydroxyl radicals above a deciduous forest canopy, J. Geophys. Res. Atmos., 106, 24315–
- 332 24 333, 2001.
- Feiner, P. A., Brune, W. H., Miller, D. O., Zhang, L., Cohen, R. C., Romer, P. S., Goldstein, A. H., Keutsch, F. N., Skog, K. M., Wennberg,
- P. O., et al.: Testing atmospheric oxidation in an Alabama forest, J. Atmos. Sci., 73, 4699–4710, 2016.
- Frisch, M. J., Trucks, G. W., Schlegel, H. B., Scuseria, G. E., Robb, M. A., Cheeseman, J. R., Scalmani, G., Barone, V., Petersson, G. A.,
- Nakatsuji, H., Li, X., Caricato, M., Marenich, A. V., Bloino, J., Janesko, B. G., Gomperts, R., Mennucci, B., Hratchian, H. P., Ortiz, J. V.,
- 337 Izmaylov, A. F., Sonnenberg, J. L., Williams-Young, D., Ding, F., Lipparini, F., Egidi, F., Goings, J., Peng, B., Petrone, A., Henderson,
- T., Ranasinghe, D., Zakrzewski, V. G., Gao, J., Rega, N., Zheng, G., Liang, W., Hada, M., Ehara, M., Toyota, K., Fukuda, R., Hasegawa,
- J., Ishida, M., Nakajima, T., Honda, Y., Kitao, O., Nakai, H., Vreven, T., Throssell, K., Montgomery, Jr., J. A., Peralta, J. E., Ogliaro, F.,
- Bearpark, M. J., Heyd, J. J., Brothers, E. N., Kudin, K. N., Staroverov, V. N., Keith, T. A., Kobayashi, R., Normand, J., Raghavachari,
- 341 K., Rendell, A. P., Burant, J. C., Iyengar, S. S., Tomasi, J., Cossi, M., Millam, J. M., Klene, M., Adamo, C., Cammi, R., Ochterski, J. W.,
- Martin, R. L., Morokuma, K., Farkas, O., Foresman, J. B., and Fox, D. J.: Gaussian ~16 Revision C.01, gaussian Inc. Wallingford CT,
- 343 2016.
- 344 Gao, Q., Shen, C., Zhang, H., Long, B., and Truhlar, D. G.: Quantitative kinetics reveal that reactions of HO<sub>2</sub> are a significant sink for
- 345 aldehydes in the atmosphere and may initiate the formation of highly oxygenated molecules via autoxidation, Phys. Chem. Phys.,
- 346 26, 16160–16174, 2024.
- 347 Geyer, A., Bächmann, K., Hofzumahaus, A., Holland, F., Konrad, S., Klüpfel, T., Pätz, H.-W., Perner, D., Mihelcic, D., Schäfer, H.-J., et al.:
- 348 Nighttime formation of peroxy and hydroxyl radicals during the BERLIOZ campaign: Observations and modeling studies, J. Geophys.
- 349 Res. Atmos., 108, 2003.
- 350 Gomez Alvarez, E., Amedro, D., Afif, C., Gligorovski, S., Schoemaecker, C., Fittschen, C., Doussin, J.-F., and Wortham, H.: Unexpectedly
- high indoor hydroxyl radical concentrations associated with nitrous acid, Proc. Natl. Acad. Sci., 110, 13 294–13 299, 2013.
- 352 Griffith, S. M., Hansen, R., Dusanter, S., Michoud, V., Gilman, J., Kuster, W., Veres, P., Graus, M., De Gouw, J., Roberts, J., et al.: Mea-
- surements of hydroxyl and hydroperoxy radicals during CalNex-LA: Model comparisons and radical budgets, J. Geophys. Res., 121,
- 354 4211–4232, 2016.
- Hall, I. W., Wayne, R. P., Cox, R. A., Jenkin, M. E., and Hayman, G. D.: Kinetics of the reaction of nitrate radical with hydroperoxo, J. Phys.
- 356 Chem., 92, 5049–5054, 1988.
- 357 Harrison, R., Yin, J., Tilling, R., Cai, X., Seakins, P., Hopkins, J., Lansley, D., Lewis, A., Hunter, M., Heard, D., et al.: Measurement and
- 358 modelling of air pollution and atmospheric chemistry in the UK West Midlands conurbation: Overview of the PUMA Consortium project,
- 359 Sci. Total Environ., 360, 5–25, 2006.
- 360 Heald, C. L. and Kroll, J. H.: A radical shift in air pollution, Science, 374, 688–689, 2021.
- 361 Heard, D., Carpenter, L., Creasey, D., Hopkins, J., Lee, J., Lewis, A., Pilling, M., Seakins, P., Carslaw, N., and Emmerson, K.: High levels of
- the hydroxyl radical in the winter urban troposphere, Geophys. Res. Lett., 31, 2004.
- Hens, K., Novelli, A., Martinez, M., Auld, J., Axinte, R., Bohn, B., Fischer, H., Keronen, P., Kubistin, D., Nölscher, A., et al.: Observation
- and modelling of HO<sub>X</sub> radicals in a boreal forest., Atmos. Chem. Phys. Discuss., 13, 2013.





- Hermans, I., Nguyen, T. L., Jacobs, P. A., and Peeters, J.: Tropopause chemistry revisited: HO<sub>2</sub>•initiated oxidation as an efficient acetone
- 366 sink, J. Am. Chem. Soc., 126, 9908–9909, 2004.
- 367 Hofzumahaus, A., Rohrer, F., Lu, K., Bohn, B., Brauers, T., Chang, C.-C., Fuchs, H., Holland, F., Kita, K., Kondo, Y., et al.: Amplified trace
- 368 gas removal in the troposphere, science, 324, 1702–1704, 2009.
- 369 Horie, O. and Moortgat, G.: Decomposition pathways of the excited Criegee intermediates in the ozonolysis of simple alkenes, Atmos.
- 370 Environ., 25A, 1881–1896, 1991.
- 371 J. Medeiros, D., Blitz, M. A., Seakins, P. W., and Whalley, L. K.: Direct measurements of isoprene autoxidation: Pinpointing atmospheric
- oxidation in tropical forests, JACS Au, 2, 809–818, 2022.
- Johnson, D. and Marston, G.: The gas-phase ozonolysis of unsaturated volatile organic compounds in the troposphere, Chem. Soc. Rev., 37,
- 374 699–716, 2008.
- 375 Johnson III, R. D.: NIST computational chemistry comparison and benchmark database, NIST standard reference database number 101,
- Release 16a http://cccbdb.nist.gov/ (accessed march 5, 2025), 2013.
- 377 Khan, M., Percival, C., Caravan, R., Taatjes, C., and Shallcross, D.: Criegee intermediates and their impacts on the troposphere, Environ.
- 378 Sci.: Process. Impacts, 20, 437–453, 2018.
- 379 Kumar, A., Mallick, S., and Kumar, P.: Nitrous acid (HONO) as a sink of the simplest Criegee intermediate in the atmosphere, Phys. Chem.
- 380 Chem. Phys., 24, 7458–7465, 2022.
- 381 Lelieveld, J., Peters, W., Dentener, F., and Krol, M.: Stability of tropospheric hydroxyl chemistry, J. Geophys. Res., 107, ACH-17, 2002.
- 382 Lelieveld, J., Dentener, F., Peters, W., and Krol, M.: On the role of hydroxyl radicals in the self-cleansing capacity of the troposphere, Atmos.
- 383 Chem. Phys., 4, 2337–2344, 2004.
- 384 Lelieveld, J., Gromov, S., Pozzer, A., and Taraborrelli, D.: Global tropospheric hydroxyl distribution, budget and reactivity, Atmos. Chem.
- 385 Phys., 16, 12477–12493, 2016.
- 386 Lelieveld, J. a., Butler, T. M., Crowley, J. N., Dillon, T. J., Fischer, H., Ganzeveld, L., Harder, H., Lawrence, M. G., Martinez, M., Taraborrelli,
- D., et al.: Atmospheric oxidation capacity sustained by a tropical forest, Nature, 452, 737–740, 2008.
- 388 Lew, M. M., Rickly, P. S., Bottorff, B. P., Reidy, E., Sklaveniti, S., Léonardis, T., Locoge, N., Dusanter, S., Kundu, S., Wood, E., et al.: OH
- and HO<sub>2</sub> radical chemistry in a midlatitude forest: measurements and model comparisons, Atmos. Chem. Phys., 20, 9209–9230, 2020.
- 390 Li, Y., Wang, X., Wu, Z., Li, L., Wang, C., Li, H., Zhang, X., Zhang, Y., Li, J., Gao, R., et al.: Atmospheric nitrous acid (HONO) in an alternate
- 391 process of haze pollution and ozone pollution in urban Beijing in summertime: Variations, sources and contribution to atmospheric
- 392 photochemistry, Atmos. Res., 260, 105 689, 2021.
- 393 Lin, H.-Y., Huang, Y.-H., Wang, X., Bowman, J. M., Nishimura, Y., Witek, H. A., and Lee, Y.-P.: Infrared identification of the Criegee
- intermediates syn-and anti-CH<sub>3</sub>CHOO, and their distinct conformation-dependent reactivity, Nat. Commun., 6, 7012, 2015.
- 395 Lin, L.-C., Chang, H.-T., Chang, C.-H., Chao, W., Smith, M. C., Chang, C.-H., Takahashi, K., et al.: Competition between H<sub>2</sub>O and (H<sub>2</sub>O)<sub>2</sub>
- reactions with CH<sub>2</sub>OO/CH<sub>3</sub>CHOO, Phys. Chem. Chem. Phys., 18, 4557–4568, 2016.
- 397 Long, B., Xia, Y., and Truhlar, D. G.: Quantitative kinetics of HO<sub>2</sub> reactions with aldehydes in the atmosphere: High-order dynamic corre-
- 398 lation, anharmonicity, and falloff effects are all important, J. Am. Chem. Soc., 144, 19910–19920, 2022.
- 399 Lu, K., Rohrer, F., Holland, F., Fuchs, H., Bohn, B., Brauers, T., Chang, C., Häseler, R., Hu, M., Kita, K., et al.: Observation and modelling
- of OH and HO<sub>2</sub> concentrations in the Pearl River Delta 2006: a missing OH source in a VOC rich atmosphere, Atmos. Chem. Phys., 12,
- 401 1541–1569, 2012.





- 402 Lu, X., Park, J., and Lin, M.-C.: Gas phase reactions of HONO with NO<sub>2</sub>, O<sub>3</sub>, and HCl: Ab initio and TST study, J. Phys. Chem. A, 104,
- 403 8730-8738, 2000.
- 404 Mallick, S. and Kumar, P.: The reaction of N<sub>2</sub>O with the Criegee intermediate: A theoretical study, Comput. Theor. Chem., 1191, 113 023,
- 405 2020
- 406 Mellouki, A., Le Bras, G., and Poulet, G.: Kinetics of the reactions of nitrate radical with hydroxyl and hydroperoxo, J. Phys. Chem. A, 92,
- 407 2229–2234, 1988.
- 408 Mellouki, A., Talukdar, R., Bopegedera, A., and Howard, C. J.: Study of the kinetics of the reactions of NO<sub>3</sub> with HO<sub>2</sub> and OH, Int. J. Chem.
- 409 Kinet., 25, 25–39, 1993.
- 410 Monks, P. S.: Gas-phase radical chemistry in the troposphere, Chem. Soc. Rev., 34, 376–395, 2005.
- 411 Novelli, A., Vereecken, L., Lelieveld, J., and Harder, H.: Direct observation of OH formation from stabilised Criegee intermediates, Phys.
- 412 Chem. Chem. Phys., 16, 19 941–19 951, 2014.
- 413 Novelli, A., Hens, K., Tatum Ernest, C., Martinez, M., Nölscher, A. C., Sinha, V., Paasonen, P., Petäjä, T., Sipilä, M., Elste, T., et al.:
- Estimating the atmospheric concentration of Criegee intermediates and their possible interference in a FAGE-LIF instrument, Atmos.
- 415 Chem. Phys., 17, 7807–7826, 2017.
- 416 Novelli, A., Vereecken, L., Bohn, B., Dorn, H.-P., Gkatzelis, G. I., Hofzumahaus, A., Holland, F., Reimer, D., Rohrer, F., Rosanka, S., et al.:
- 417 Importance of isomerization reactions for OH radical regeneration from the photo-oxidation of isoprene investigated in the atmospheric
- simulation chamber SAPHIR, Atmos. Chem. Phys., 20, 3333–3355, 2020.
- 419 Onel, L., Lade, R., Mortiboy, J., Blitz, M. A., Seakins, P. W., Heard, D. E., and Stone, D.: Kinetics of the gas phase reaction of the Criegee
- intermediate CH<sub>2</sub>OO with SO<sub>2</sub> as a function of temperature, Phys. Chem. Chem. Phys., 23, 19415–19423, 2021.
- 421 Osborn, D. L. and Taatjes, C. A.: The physical chemistry of Criegee intermediates in the gas phase, Int. Rev. Phys. Chem., 34, 309-360,
- 422 2015.
- 423 Østerstrøm, F. F., Carter, T. J., Shaw, D. R., Abbatt, J. P., Abeleira, A., Arata, C., Bottorff, B. P., Cardoso-Saldaña, F. J., DeCarlo, P. F.,
- 424 Farmer, D. K., et al.: Modelling indoor radical chemistry during the HOMEChem campaign, Environ. Sci.: Process. Impacts, 2025.
- 425 Pansini, F., Neto, A., and Varandas, A.: Extrapolation of Hartree-Fock and multiconfiguration self-consistent-field energies to the complete
- 426 basis set limit, Theor. Chem. Acc., 135, 1–6, 2016.
- 427 Paulot, F., Crounse, J. D., Kjaergaard, H. G., Kürten, A., St. Clair, J. M., Seinfeld, J. H., and Wennberg, P. O.: Unexpected epoxide formation
- in the gas-phase photooxidation of isoprene, science, 325, 730–733, 2009.
- 429 Pawar, P. V., Mahajan, A. S., and Ghude, S. D.: HONO chemistry and its impact on the atmospheric oxidizing capacity over the Indo-Gangetic
- 430 Plain, Sci. Total Environ., p. 174604, 2024.
- 431 Peeters, J. and Mu'ller, J.-F.:  $HO_X$  radical regeneration in isoprene oxidation via peroxy radical isomerisations. II: experimental evidence
- 432 and global impact, Phys. Chem. Chem. Phys., 12, 14 227–14 235, 2010.
- 433 Peeters, J., Nguyen, T. L., and Vereecken, L.: HO<sub>X</sub> radical regeneration in the oxidation of isoprene, Phys. Chem. Chem. Phys., 11, 5935–
- 434 5939, 2009.
- 435 Peeters, J., Muller, J.-F., Stavrakou, T., and Nguyen, V. S.: Hydroxyl radical recycling in isoprene oxidation driven by hydrogen bonding and
- 436 hydrogen tunneling: The upgraded LIM1 mechanism, J. Phys. Chem. A, 118, 8625–8643, 2014.
- 437 Prinn, R. G.: The Cleansing Capacity of the Atmosphere, Annu. Rev. Environ. Resour., 28, 29–57, 2003.
- 438 Rai, P. K. and Kumar, P.: Mechanistic Inside into the Gas-Phase NO<sub>3</sub> + HO<sub>2</sub> Reaction, J. Phys. Chem. A, 128, 7907–7913, 2024.
- 439 Rai, P. K. and Kumar, P.: Influence of Water on the NO<sub>3</sub> + HO<sub>2</sub> Reaction, J. Phys. Chem. A, 129, 2067–2076, 2025.





- 440 Reidy, E., Bottorff, B. P., Rosales, C. M. F., Cardoso-Saldaña, F. J., Arata, C., Zhou, S., Wang, C., Abeleira, A., Hildebrandt Ruiz, L.,
- 441 Goldstein, A. H., et al.: Measurements of hydroxyl radical concentrations during indoor cooking events: Evidence of an unmeasured
- photolytic source of radicals, Environ. Sci. Technol., 57, 896–908, 2023.
- 443 Ren, X., Harder, H., Martinez, M., Lesher, R. L., Oliger, A., Shirley, T., Adams, J., Simpas, J. B., and Brune, W. H.: HO<sub>X</sub> concentrations
- and OH reactivity observations in New York City during PMTACS-NY2001, Atmos. Environ., 37, 3627–3637, 2003.
- 445 Ruscic, B., Pinzon, R. E., Morton, M. L., von Laszevski, G., Bittner, S. J., Nijsure, S. G., Amin, K. A., Minkoff, M., and Wagner, A. F.:
- Introduction to active thermochemical tables: Several "key" enthalpies of formation revisited, J. Phys. Chem. A, 108, 9979–9997, 2004.
- 447 Sander, R., Baumgaertner, A., Cabrera-Perez, D., Frank, F., Gromov, S., Grooß, J.-U., Harder, H., Huijnen, V., Jöckel, P., Karydis, V. A.,
- et al.: The community atmospheric chemistry box model CAABA/MECCA-4.0, Geosci. Model Dev., 12, 1365–1385, 2019.
- 449 Shabin, M., Kumar, A., Hakkim, H., Rudich, Y., and Sinha, V.: Sources, sinks, and chemistry of stabilized Criegee intermediates in the
- indo-gangetic plain, Sci. Total Environ., 896, 165 281, 2023.
- 451 Sheps, L., Scully, A. M., and Au, K.: UV absorption probing of the conformer-dependent reactivity of a Criegee intermediate CH<sub>3</sub>CHOO,
- 452 Phys. Chem. Chem. Phys., 16, 26701–26706, 2014.
- 453 Slater, E. J., Whalley, L. K., Woodward-Massey, R., Ye, C., Lee, J. D., Squires, F., Hopkins, J. R., Dunmore, R. E., Shaw, M., Hamilton, J. F.,
- et al.: Elevated levels of OH observed in haze events during wintertime in central Beijing, Atmos. Chem. Phys., 20, 14 847–14 871, 2020.
- 455 Smith, M. C., Chao, W., Takahashi, K., Boering, K. A., and Lin, J. J.-M.: Unimolecular decomposition rate of the Criegee intermediate
- 456 (CH<sub>3</sub>)<sub>2</sub>COO measured directly with UV absorption spectroscopy, J. Phys. Chem. A, 120, 4789–4798, 2016.
- 457 Smith, S., Lee, J., Bloss, W., Johnson, G., Ingham, T., and Heard, D.: Concentrations of OH and HO<sub>2</sub> radicals during NAMBLEX: measure-
- 458 ments and steady state analysis, Atmos. Chem. Phys., 6, 1435–1453, 2006.
- 459 Song, M., Zhao, X., Liu, P., Mu, J., He, G., Zhang, C., Tong, S., Xue, C., Zhao, X., Ge, M., et al.: Atmospheric NO<sub>X</sub> oxidation as major
- sources for nitrous acid (HONO), npj clim. atmos. sci., 6, 30, 2023.
- 461 Stone, D., Whalley, L. K., and Heard, D. E.: Tropospheric OH and HO<sub>2</sub> radicals: field measurements and model comparisons, Chem. Soc.
- 462 Rev., 41, 6348–6404, 2012.
- 463 Taatjes, C. A.: Criegee intermediates: What direct production and detection can teach us about reactions of carbonyl oxides, Annu. Rev.
- 464 Phys. Chem., 68, 183–207, 2017.
- 465 Tan, D., Faloona, I., Simpas, J., Brune, W., Shepson, P., Couch, T., Sumner, A., Carroll, M., Thornberry, T., Apel, E., et al.: HO<sub>X</sub> budgets in
- 466 a deciduous forest: Results from the PROPHET summer 1998 campaign, J. Geophys. Res. Atmos., 106, 24407–24427, 2001.
- 467 Tan, Z., Fuchs, H., Lu, K., Hofzumahaus, A., Bohn, B., Broch, S., Dong, H., Gomm, S., Häseler, R., He, L., et al.: Radical chemistry at a
- rural site (Wangdu) in the North China Plain: observation and model calculations of OH, HO<sub>2</sub> and RO<sub>2</sub> radicals, Atmos. Chem. Phys., 17,
- 469 663–690, 2017.
- 470 Teng, A. P., Crounse, J. D., and Wennberg, P. O.: Isoprene peroxy radical dynamics, J. Am. Chem. Soc., 139, 5367–5377, 2017.
- 471 Varandas, A. and Pansini, F.: Narrowing the error in electron correlation calculations by basis set re-hierarchization and use of the unified
- singlet and triplet electron-pair extrapolation scheme: Application to a test set of 106 systems, J. Chem. Phys., 141, 224 113, 2014.
- 473 Vereecken, L. and Francisco, J. S.: Theoretical studies of atmospheric reaction mechanisms in the troposphere, Chem. Soc. Rev., 41, 6259-
- 474 6293, 2012
- 475 Vereecken, L., Harder, H., and Novelli, A.: The reaction of Criegee intermediates with NO, RO<sub>2</sub>, and SO<sub>2</sub>, and their fate in the atmosphere,
- 476 Phys. Chem. Chem. Phys., 14, 14682–14695, 2012.





- 477 Vereecken, L., Rickard, A., Newland, M., and Bloss, W.: Theoretical study of the reactions of Criegee intermediates with ozone, alkylhy-
- 478 droperoxides, and carbon monoxide, Phys. Chem. Chem. Phys., 17, 23 847–23 858, 2015.
- 479 Vereecken, L., Novelli, A., and Taraborrelli, D.: Unimolecular decay strongly limits the atmospheric impact of Criegee intermediates, Phys.
- 480 Chem. Chem. Phys., 19, 31 599–31 612, 2017.
- 481 Viegas, L. P. and Varandas, A. J.: Can water be a catalyst on the HO<sub>2</sub> + H<sub>2</sub>O + O<sub>3</sub> reactive cluster?, Chem. Phys., 399, 17–22, 2012.
- Wallington, T. J. and Japar, S. M.: Fourier transform infrared kinetic studies of the reaction of HONO with HNO $_3$ , NO $_3$  and N $_2$ O $_5$  at 295 K,
- 483 J. Atmos. Chem., 9, 399–409, 1989.
- 484 Weinstock, B.: Carbon monoxide: Residence time in the atmosphere, Science, 166, 224–225, 1969.
- Whalley, L., Edwards, P., Furneaux, K., Goddard, A., Ingham, T., Evans, M. J., Stone, D., Hopkins, J., Jones, C. E., Karunaharan, A., et al.:
- Quantifying the magnitude of a missing hydroxyl radical source in a tropical rainforest, Atmos. Chem. Phys., 11, 7223–7233, 2011.
- 487 Yang, X., Wang, H., Lu, K., Ma, X., Tan, Z., Long, B., Chen, X., Li, C., Zhai, T., Li, Y., et al.: Reactive aldehyde chemistry explains the
- 488 missing source of hydroxyl radicals, Nat. Commun., 15, 1648, 2024.
- 489 Zhang, N., Zhou, X., Bertman, S., Tang, D., Alaghmand, M., Shepson, P., and Carroll, M.: Measurements of ambient HONO concentrations
- and vertical HONO flux above a northern Michigan forest canopy, Atmos. Chem. Phys., 12, 8285–8296, 2012.
- 491 Zhang, Q., Tie, X., Lin, W., Cao, J., Quan, J., Ran, L., and Xu, W.: Variability of SO<sub>2</sub> in an intensive fog in North China Plain: Evidence of
- high solubility of SO<sub>2</sub>, Particuology, 11, 41–47, 2013.





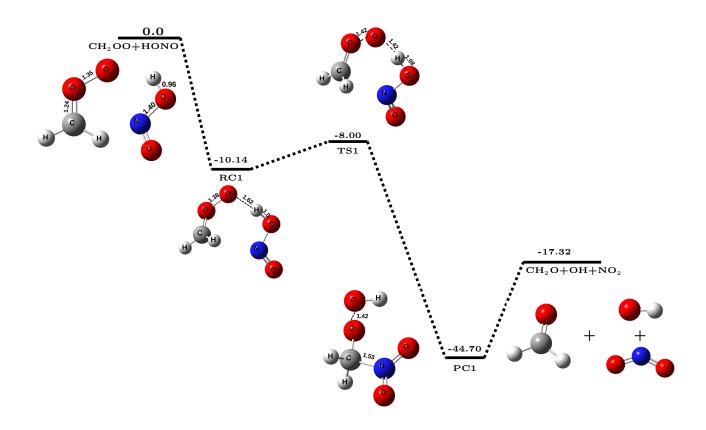


Figure 1. The potential energy surface for  $CH_2OO + HONO$  reaction (in kcal  $mol^{-1}$ ) obtained at CCSD(T)/CBS//M06-2X/aug-cc-pVTZ level of theory along with optimized geometries of species involved in the reaction.





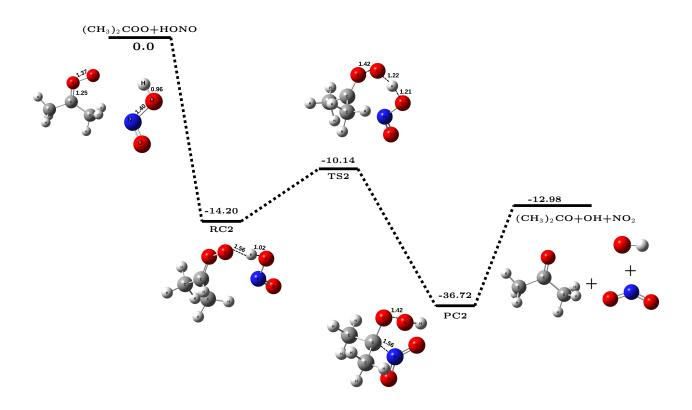


Figure 2. The potential energy surface for  $(CH_3)_2COO + HONO$  reaction (in kcal mol<sup>-1</sup>) obtained at CCSD(T)/CBS//M06-2X/aug-cc-pVTZ level of theory along with optimized geometries of species involved in the reaction.





**Table 1.** Bimolecular rate constants ( $k_{bi}$ , in cm<sup>3</sup> molecule<sup>-1</sup> sec<sup>-1</sup>) for CH<sub>2</sub>OO/(CH<sub>3</sub>)<sub>2</sub>COO + HONO reaction within the temperature range of 213–320 K.

T (K)	$\mathbf{k}_{bi}^{CH_{2}OO}$	$\mathbf{k}_{bi}^{(CH_3)_2COO}$
213	$3.94 \times 10^{-12}$	$2.17 \times 10^{-11}$
216	$3.94 \times 10^{-12}$	$2.23 \times 10^{-11}$
219	$3.94 \times 10^{-12}$	$2.28 \times 10^{-11}$
224	$3.93 \times 10^{-12}$	$2.38 \times 10^{-11}$
235	$3.90 \times 10^{-12}$	$2.57 \times 10^{-11}$
250	$3.83 \times 10^{-12}$	$2.83 \times 10^{-11}$
259	$3.76 \times 10^{-12}$	$2.97 \times 10^{-11}$
265	$3.71 \times 10^{-12}$	$3.06 \times 10^{-11}$
278	$3.58 \times 10^{-12}$	$3.24 \times 10^{-11}$
280	$3.56 \times 10^{-12}$	$3.26 \times 10^{-11}$
290	$3.45 \times 10^{-12}$	$3.38 \times 10^{-11}$
298	$3.35 \times 10^{-12}$	$3.46 \times 10^{-11}$
300	$3.33 \times 10^{-12}$	$3.47 \times 10^{-11}$
310	$3.20 \times 10^{-12}$	$3.56 \times 10^{-11}$
320	$3.06 \times 10^{-12}$	$3.62 \times 10^{-11}$





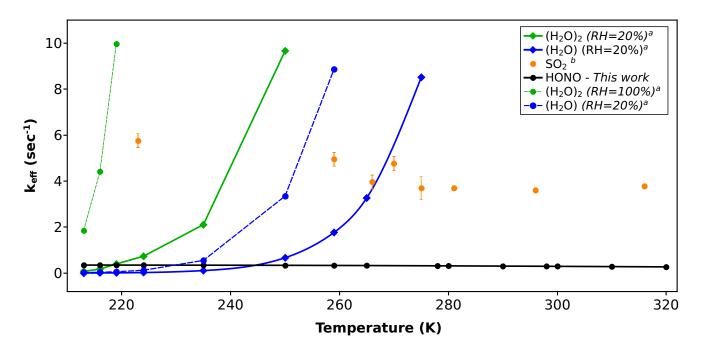
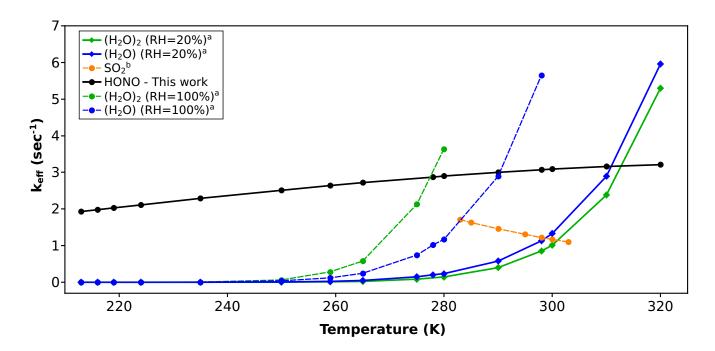


Figure 3. Effective rate constant comparison  $(k_{eff}, \text{ in sec}^{-1})$  of  $CH_2OO + HONO$  with the  $k_{eff}$  of previously known sinks of  $CH_2OO$ . a. Values are taken from reference (Lin et al., 2016)

b. Values are taken from reference (Onel et al., 2021)







**Figure 4.** Effective rate constant comparison  $(k_{eff}, \text{ in sec}^{-1})$  of  $(CH_3)_2COO + HONO$  with the  $k_{eff}$  of previously known sinks of  $(CH_3)_2COO$ .

- a. Values are taken from reference (Vereecken et al., 2017)
- b. Values are taken from reference (Smith et al., 2016)





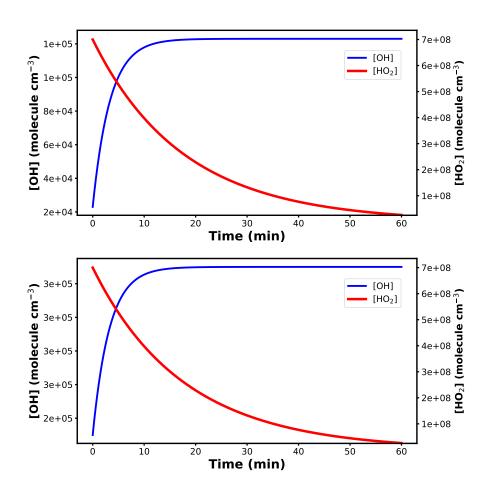


Figure 5. Top panel: Concentration profiles of  $HO_2^{\bullet}$  and  $OH^{\bullet}$  using  $CH_2OO + HONO$  reaction into the model. Bottom panel: Concentration profiles of  $HO_2^{\bullet}$  and  $OH^{\bullet}$  using  $(CH_3)_2COO + HONO$  reaction into the model.